The EMBO Journal (2005) 24, 3747–3756 | © 2005 European Molecular Biology Organization | All Rights Reserved 0261-4189/05
www.embojournal.org

THE EMBO JOURNAL

Structure and mechanisms of the proteasome-associated deubiquitinating enzyme USP14

Min Hu[1,4], Pingwei Li[1,4], Ling Song[2], Philip D Jeffrey[1], Tatiana A Chernova[3], Keith D Wilkinson[3], Robert E Cohen[2] and Yigong Shi[1,*]

[1]Department of Molecular Biology, Lewis Thomas Laboratory, Princeton University, Princeton, NJ, USA, [2]Department of Biochemistry, University of Iowa, Iowa City, IA, USA and [3]Department of Biochemistry, Emory University School of Medicine, Atlanta, GA, USA

The ubiquitin-specific processing protease (UBP) family of deubiquitinating enzymes plays an essential role in numerous cellular processes. Mammalian USP14 (Ubp6 in yeast) is unique among known UBP enzymes in that it is activated catalytically upon specific association with the 26S proteasome. Here, we report the crystal structures of the 45-kDa catalytic domain of USP14 in isolation and in a complex with ubiquitin aldehyde, which reveal distinct structural features. In the absence of ubiquitin binding, the catalytic cleft leading to the active site of USP14 is blocked by two surface loops. Binding by ubiquitin induces a significant conformational change that translocates the two surface loops thereby allowing access of the ubiquitin C-terminus to the active site. These structural observations, in conjunction with biochemical characterization, identify important regulatory mechanisms for USP14.

The EMBO Journal (2005) **24,** 3747–3756. doi:10.1038/sj.emboj.7600832; Published online 6 October 2005
Subject Categories: proteins; structural biology
Keywords: crystal structure; deubiquitination; deubiquitinating enzymes; mechanism; UBP

Introduction

Protein ubiquitination plays an essential role in the regulation of many cellular processes in eukaryotes (Hershko *et al*, 2000; Glickman and Ciechanover, 2002; Pickart, 2004). Ubiquitin is a highly conserved 76-amino-acid polypeptide. Through sequential action of three classes of enzymes known as ubiquitin-activating enzyme (E1), ubiquitin-conjugating enzymes (E2), and ubiquitin ligases (E3), ubiquitin is linked to target proteins by an isopeptide bond between the C-terminal carboxylate group of ubiquitin and the lysine ε-amino group of the acceptor protein. Ubiquitination is tightly regulated, and aberrations in this pathway are known to lead to a variety of clinical disorders (Schwartz and Ciechanover, 1999; Chung *et al*, 2001). A major function of ubiquitination is to target proteins for degradation by the 26S proteasome.

Protein deubiquitination has been identified as an important regulatory step in the ubiquitin-dependent pathways (D'Andrea and Pellman, 1998; Wilkinson *et al*, 2000; Kim *et al*, 2003; Wing, 2003; Amerik and Hochstrasser, 2004). Deubiquitination is carried out by the deubiquitinating enzymes (DUBs), which catalyze the hydrolysis of the isopeptide bond in ubiquitin–protein conjugates. There are at least five conserved families of DUBs, of which the ubiquitin-specific processing proteases (UBPs) is the largest, with more than 60 members identified in the human genome.

The 26S proteasome is a multi-subunit machine that degrades polyubiquitinated protein substrates (Zwickl *et al*, 1999; Pickart and Cohen, 2004). A number of auxiliary proteins, such as ubiquitinating enzymes (Verma *et al*, 2000; Xie and Varshavsky, 2000) and DUBs (Lam *et al*, 1997; Papa *et al*, 1999; Verma *et al*, 2000; Borodovsky *et al*, 2001; Leggett *et al*, 2002; Guterman and Glickman, 2004b), specifically associate with the proteasome. The proteasome-associated DUBs include UCH37 (Lam *et al*, 1997), a member of the UCH family, POH1/Rpn11, an MPN + /JAMM domain metalloprotease (Verma *et al*, 2002; Yao and Cohen, 2002), and USP14/Ubp6 (Borodovsky *et al*, 2001; Leggett *et al*, 2002; Chernova *et al*, 2003), a member of the UBP family. These DUBs help to remove the (poly)ubiquitin moiety from protein substrates before or during translocation into the catalytic chamber of the proteasome for degradation. The editing function of DUBs can rescue poorly ubiquitinated protein substrates from degradation by the 26S proteasome (Lam *et al*, 1997), whereas the ubiquitin-recycling function is critical for maintaining the free ubiquitin pool in cells and protects the proteasome from being jammed by the ubiquitin chains attached to substrates (Leggett *et al*, 2002; Verma *et al*, 2002; Yao and Cohen, 2002; Chernova *et al*, 2003; Hanna *et al*, 2003; Guterman and Glickman, 2004a). Both USP14 and Ubp6 contain a ubiquitin-like (Ubl) domain at the N-terminus (Wyndham *et al*, 1999); the Ubl of Ubp6 has been shown to be responsible for the association with 26S proteasomes. This association results in the dramatic enhancement of Ubp6 deubiquitinating activity *in vitro*, although the underlying mechanism remains unclear (Leggett *et al*, 2002).

Mutations that eliminate Rpn11 deubiquitinating activity are lethal for yeast and lead to the accumulation of ubiquitinated degradation substrates (Verma *et al*, 2002; Yao and Cohen, 2002). Lesions in the proteasome-associated UBP enzyme, USP14/Ubp6, have pronounced but milder effects. In mice, defective USP14 results in abnormal synaptic transmission and ataxia (Wilson *et al*, 2002). In budding yeast, deletion of *UBP6* severely impairs growth under various conditions of stress and causes a major depletion of the cellular ubiquitin pool; indeed, ubiquitin overexpression can suppress the phenotypes of *ubp6*Δ yeast (Chernova *et al*, 2003; Hanna *et al*, 2003). Although both POH1/Rpn11 and USP14/Ubp6 function to recycle ubiquitin, the more

*Corresponding author. Department of Molecular Biology, Lewis Thomas Laboratory, Princeton University, Princeton, NJ 08544, USA. Tel.: +1 609 258 6071; Fax: +1 609 258 6730;
E-mail: yshi@molbio.princeton.edu
[4]These authors contributed equally to this work

Received: 11 July 2005; accepted: 12 September 2005; published online: 6 October 2005

drastic effects of mutations in POH1/Rpn11 suggest that it bears the greater responsibility for releasing ubiquitin from proteasomal substrates. Nonetheless, *rpn11* and *ubp6* mutations are synthetically lethal in yeast (Guterman and Glickman, 2004a), which suggests that these structurally very distinct DUBs have overlapping functions. Understanding how these DUBs are regulated and how their substrates are identified is a major unsolved problem in the area of ubiquitin-dependent degradation.

The UBPs are cysteine proteases that contain highly divergent sequences and exhibit strong homology mainly in two regions that surround the catalytic Cys and His residues; these are the so-called Cys Box (~19 amino acids) and the His Box (60–90 amino acids) (Papa and Hochstrasser, 1993; D'Andrea and Pellman, 1998). The structure of the catalytic core domain of HAUSP (also known as USP7) revealed a tripartite architecture comprising Fingers, Palm, and Thumb domains (Hu *et al*, 2002). Given the highly divergent sequences and scarce structural information, it is unclear whether this three-domain architecture is generally conserved among other UBPs. In addition, the catalytic residues in HAUSP are mis-aligned before substrate binding. Binding by ubiquitin aldehyde (Ubal) induces a drastic conformational change in the active site that realigns the catalytic triad residues for catalysis (Hu *et al*, 2002). It is unknown whether this is a general activation mechanism among UBPs.

In this manuscript, we report the crystal structures of the 45-kDa catalytic domain of USP14 in isolation and in a complex with ubiquitin aldehyde. We show that, despite a conserved three-domain architecture, the activation mechanism for USP14 is quite different from that for HAUSP. We also present important biochemical data on the function and regulation of USP14.

Results

Structure of the USP14 catalytic domain

The full-length human USP14 contains 494 amino acids, with a 9-kDa Ubl domain at its N-terminus followed by a 45-kDa catalytic domain. To investigate the function and catalytic mechanism of USP14, we crystallized and determined the structure of the USP14 catalytic domain (residues 91–494) at 3.2 Å resolution using multiwavelength anomalous dispersion (Table I and Figure 1A). In the crystals, there are three molecules of USP14 per asymmetric unit, which have a pairwise root-mean-square deviation (RMSD) of approximately 1 Å. These three molecules exhibit identical structural features important for this discussion. Hence, for simplicity, we limit our discussion to one such molecule.

Similar to HAUSP (Hu *et al*, 2002), the catalytic domain of USP14 resembles an extended right hand comprised of three domains: Fingers, Palm, and Thumb (Figures 1 and 2). The three-domain organization creates a prominent binding surface between the Fingers and the Palm–Thumb scaffold, which is predicted to bind to ubiquitin. The Thumb contains 6α helices (α1–α6) and one short β strand (β1), with the N-terminal Cys Box adopting an extended conformation. The Palm consists of a six-stranded (β5, β8, β10–β13) central β sheet, three α helices (α7–α9), one short β strand (β9), and several surface loops. Notably, two surface loops hover above and partially fill the predicted binding pocket for the C-terminus of ubiquitin (Figure 1A). These two loops are named blocking loops 1 and 2 (BL1 and BL2; Figures 1B and 2). The Fingers comprise five β strands (β2–β4, β6, and β7). In contrast to the HAUSP structure (Hu *et al*, 2002), packing interactions between the central β sheet in the Palm and the globular Thumb do not give rise to an interdomain cleft

Table I Summary of crystallographic analysis

Data sets	Native (USP14)	Native (USP14–Ubal)	Peak (Se1)	Inflection (Se2)	Remote (Se3)
Wavelength (Å)	1.10	0.976	0.9793	0.9795	0.9500
Space group	P212121	P3121	P212121	P212121	P212121
Resolution (Å)	99–3.2	99–3.5	99–3.35	99–3.35	99–3.35
Unique reflections	27 320	11 099	24 378	24 012	24 805
Completeness (outer shell)	98.9% (96.3%)	98.0% (92.8%)	99.7% (98.6%)	99.8% (99.4%)	99.7% (99.1%)
R_{sym} (outer shell)[a]	0.078 (0.53)	0.117 (0.54)	0.143 (0.72)	0.123 (0.67)	0.132 (0.77)
Data redundancy	5.6	3.3	9.6	7.2	7.2
Average I/σ (outer shell)	26.4 (2.8)	10.9 (2.0)	19.5 (2.8)	17.8 (2.6)	16.6 (2.2)
Anomalous difference (%)			11.9	10.0	10.6
Cullis *R*-factor			0.58	0.60	0.66
Phasing power (centric/acentric)			2.56/1.84	2.36/1.75	1.79/1.29
Mean figure of merit (20–3.35 Å)			0.48		

Refinement statistics

Resolution range (Å)	Number of reflections	Total number of atoms	Completeness of data (outer shell)	*R*-factor[b] (*R*-free)	RMSD[c]	
					Bond (Å)	Angle (deg)
99–3.2 (USP14)	25 614 ($\|F\|>\sigma$)	8166	90.1% (83.4%)	0.261 (0.322)	0.011	1.56
99–3.5 (USP14–Ubal)	11 095 ($\|F\|>0$)	3412	97.9% (96.1%)	0.29 (0.33)	0.013	1.91

[a]$R_{sym}=\sum_h\sum_i|I_{h,i}-I_h|/\sum_h\sum_i I_{h,i}$, where I_h is the mean intensity of the i observations of symmetry-related reflections of h.
[b]$R=\sum|F_{obs}-F_{calc}|/\sum F_{obs}$, where $F_{obs}=F_P$, and F_{calc} is the calculated protein structure factor from the atomic model (R_{free} was calculated with 5% of the reflections).
[c]RMSD (root-mean-square deviation) in bond lengths and angles are the deviations from ideal values.

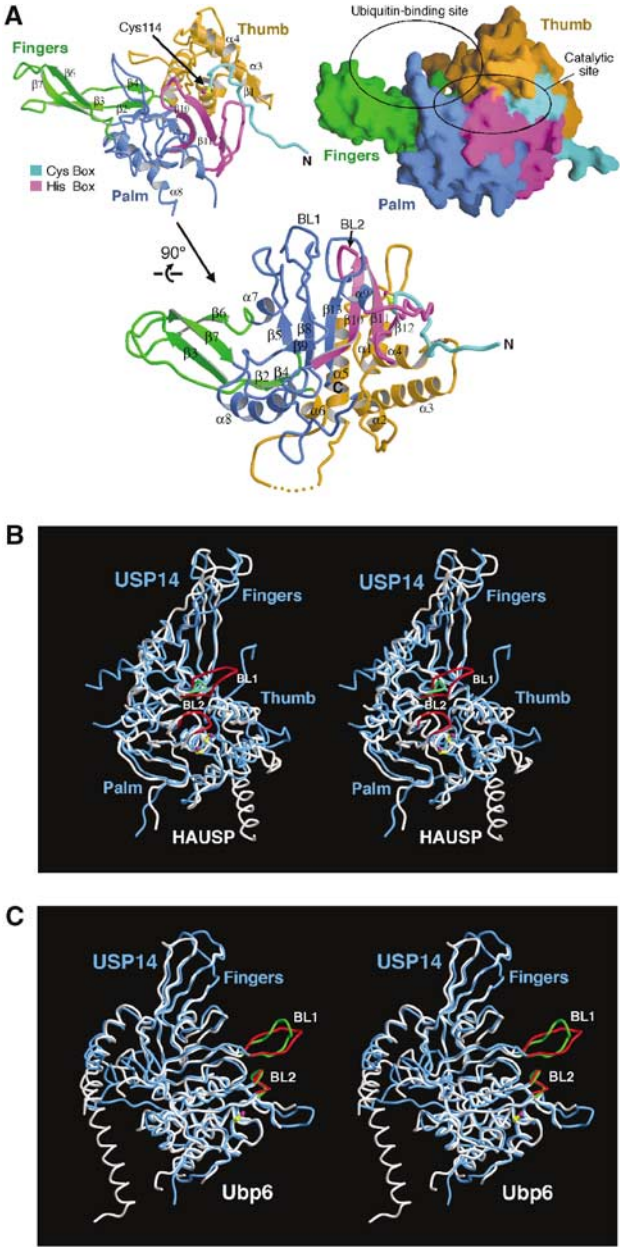

Figure 1 Structure of the catalytic domain of USP14. (**A**) Overall structure of the 45-kDa catalytic domain of USP14 (residues 91–494). The structure comprises three domains, Fingers (in green), Palm (in blue), and Thumb (in gold). The active site, comprising the Cys Box (in cyan) and the His Box (in magenta), is located between the Palm and the Thumb. The predicted ubiquitin-binding site is indicated by a black oval circle. The surface representation is shown on the right. Note the absence of the binding groove for the C-terminus of ubiquitin. (**B**) Comparison of the structures of the catalytic domain between USP14 and HAUSP in a stereo view. USP14 and HAUSP are shown in blue and white, respectively. The active site of free USP14 is covered by two crossover loops BL1 and BL2 (in red). The catalytic Cys residues in USP14 and HAUSP are highlighted in yellow. (**C**) Comparison of the structures of the catalytic domain between USP14 and Ubp6 in a stereo view. Note that two surface loops (green) in Ubp6 adopt very similar positions as the BL1 and BL2 loops (red) in USP14. All figures were prepared using MOLSCRIPT (Kraulis, 1991) and GRASP (Nicholls *et al*, 1991).

between the Palm and the Thumb (Figure 1A, right panel), which is needed for the accommodation of ubiquitin C-terminus.

The structure of the USP14 catalytic domain resembles that of the HAUSP catalytic core domain (Hu *et al*, 2002), with an RMSD of 1.7 Å for 238 aligned backbone Cα atoms (Figure 1B). Given only 13.9% sequence identity between USP14 and HAUSP (Figure 2), the preservation of the three-domain architecture suggests that this organization may be generally conserved among all members of the UBP family of proteins. In support of this conclusion, all residues that directly contribute to the structural integrity of the Fingers, Palm, and the Thumb are highly conserved among HAUSP, USP14, Ubp6, and other representative UBPs (Figure 2) (Hu *et al*, 2002).

Despite overall structural similarity, USP14 and HAUSP exhibit a number of significant local structural differences (Figures 1B and 2). Compared to HAUSP, USP14 contains one additional α helix (α8) in the Palm domain and a few extended surface loops in the Thumb and Palm domains, but is missing two C-terminal helices. In addition, a short β strand (β13) in the His Box of the HAUSP core domain structure is replaced by a surface loop in USP14. There are also apparent local structural differences in the Fingers domain. Two extended strands β1 and β2 in the HAUSP structure are replaced by a pair of short β strands (β2 and β3) followed by a surface loop and a short strand β4 in USP14. Moreover, two short β strands (β4 and β5) in HAUSP are reduced to a loop conformation in USP14.

Ubp6 is the functional homolog of USP14 in *Saccharomyces cerevisiae* and shares 31% sequence identity with USP14 in the catalytic core domain. Thus, it is not surprising that the structure of the USP14 catalytic domain is also very similar to that of the catalytic core domain from Ubp6 (www.rcsb.org, accession code 1VJV), with an RMSD of 1.2 Å for 288 aligned backbone Cα atoms. Interestingly, similar to USP14, Ubp6 contains two surface loops that are located above and partially block the predicted binding pocket for the C-terminus of ubiquitin (Figure 1C). These two surface loops exhibit nearly identical topology as BL1 and BL2 in USP14 (Figure 1C). In contrast to the USP14–HAUSP comparison, the local structural differences between USP14 and Ubp6 concentrate in surface regions whereas the core structural elements are nearly identical to each other (Figure 1C).

Active site conformation

One of the most striking features revealed by the structure of the isolated HAUSP catalytic core domain is the mis-aligned active site (Hu *et al*, 2002). In the free HAUSP structure, the catalytic histidine (His464) is nearly 10 Å away from the catalytic cysteine (Cys223), which is too far for any meaningful interaction. In contrast to the deformed active site conformation of HAUSP, the active site of free USP14 is already well formed before substrate binding (Figure 3A). Superposition of the active sites between HAUSP and USP14 revealed striking differences (Figure 3B). The $N_{\delta 1}$ atom in the imidazole ring of the candidate catalytic histidine (His435) is approximately 3.3 Å away from the S_{γ} atom in the side chain of the catalytic cysteine (Cys114), consistent with a hydrogen bond distance. A third residue, Asp451, stabilizes His435 by accepting a hydrogen bond from its $N_{\varepsilon 1}$ atom. Thus, Cys114, His435, and Asp451 form a catalytic triad in the active site of free USP14, and the catalytic mechanism of USP14 appears to parallel that of the papain family of cysteine proteases.

Figure 2 Sequence alignment of USP14 with its yeast homolog Ubp6 and human HAUSP. Conserved residues are shaded in yellow whereas the catalytic triad residues are highlighted in red. The secondary structural elements above the sequences are indicated for free USP14 (lower) and HAUSP (upper). The four black arrowheads indicate the positions where Cys residues are supposed to be located in a zinc ribbon (Krishna and Grishin, 2004). The coloring scheme for the secondary structural elements of free USP14 is the same as in Figure 1. Sequence alignment employed the program ClustalW. Entries shown are from the SwissProt Database: HAUSP (Human; SW:Q93009); USP14 (Human; SW:P54578); UBP6 (*S. cerevisiae*; SW:P35127).

The fact that the catalytic triad residues in free USP14 exist in a productive conformation suggests that free USP14 is already poised for catalysis. This conclusion is in contrast to the observation that free USP14 exhibits only a low level of deubiquitinating activity toward substrates and weak reactivity with ubiquitin vinylsulfone (UbVS, see below). An examination of the USP14 structure reveals a plausible explanation. Although the catalytic triad residues already adopt a productive conformation, access to these residues by ubiquitin is restricted (Figure 3C). Right above the active site of USP14, the two surface loops BL2 and BL1 are positioned very close to the predicted binding groove for the C-terminus of ubiquitin. Superposition of USP14 with the HAUSP–Ubal complex revealed that loops BL2 and BL1 would likely block access of the C-terminus of ubiquitin to the active site of USP14. Thus, the blockade of the ubiquitin C-terminus binding groove by loops BL2 and BL1 must be removed in order for USP14 to catalyze deubiquitination.

Consistent with this analysis, the active site of the yeast Ubp6 protein (www.rcsb.org, accession code 1VJV) adopts a highly similar conformation to that of USP14 (Figure 3D). The catalytic triad residues in Ubp6, Cys118, His447, and Asn465, can be superimposed with those from USP14 with an RMSD of 0.1 Å. The $N_{\delta 1}$ atom in the imidazole ring of His447 is within hydrogen bond distance of the side chain of Cys118, and this interaction is buttressed by a second hydrogen bond from Asn465 to His447 (Figure 3D). Thus, the catalytic triad residues Cys118, His447, and Asn465 in Ubp6 already exist in a productive conformation. Similar to USP14, this observation suggests that the blockade of the ubiquitin C-terminus binding groove by two surface loops should be removed before Ubp6 can catalyze deubiquitination.

Overall structure of USP14–Ubal complex

Ubal is a ubiquitin derivative in which the C-terminal carboxylate is replaced by an aldehyde. Ubal is a potent covalent

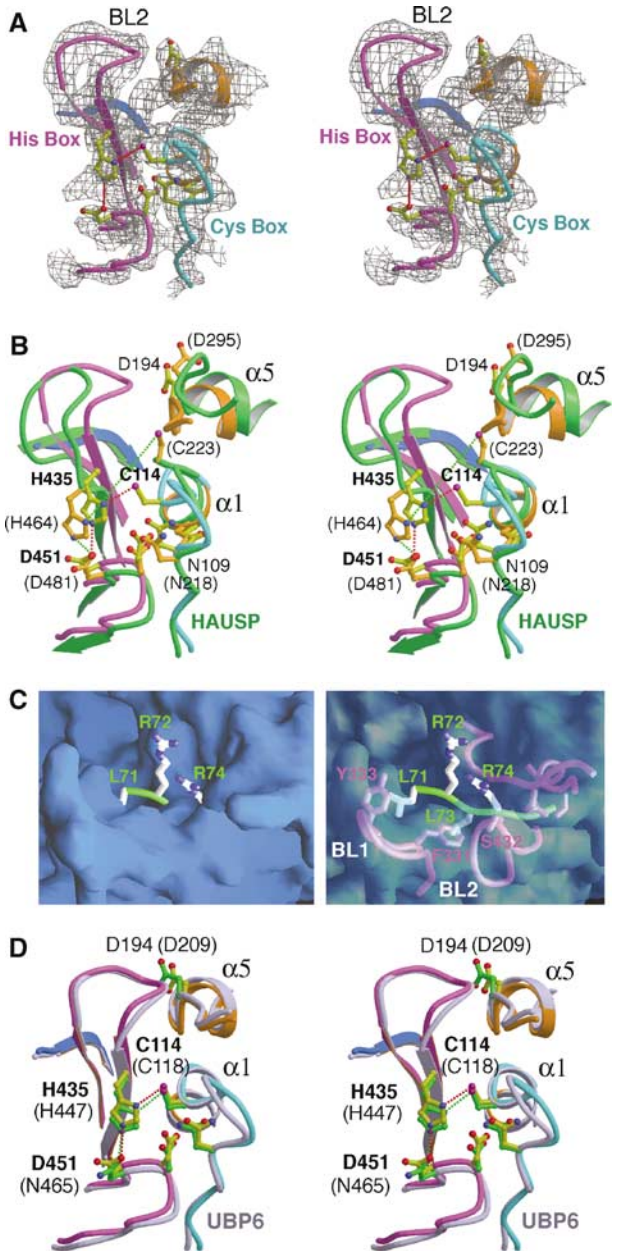

Figure 3 The active site of USP14. (**A**) The $2F_o-F_c$ electron density at the active site region contoured at 1.8σ. The Cys and His Boxes are colored cyan and magenta, respectively. (**B**) The catalytic triad residues of USP14 are poised for catalysis. Shown here is a stereo comparison of the active sites of USP14 and HAUSP. The coloring scheme for USP14 is the same as in Figure 1. HAUSP is shown in green. Catalytic triad residues and the oxyanion-coordinating residue are shown. Hydrogen bonds are represented by red dashed lines. (**C**) The binding cleft for the C-terminus of ubiquitin is blocked by two surface loops in USP14. The binding region for the C-terminus of ubiquitin is shown in two surface representations: solid (left panel) and transparent (right panel). The C-terminus of ubiquitin (green) is placed after superposition of the HAUSP–Ubal structure onto USP14. Several residues of USP14, including Phe331, Tyr333, and Ser432, sterically clash with the C-terminus of ubiquitin. (**D**) Comparison of the active site conformation in USP14 and Ubp6. Residues from USP14 are labeled, whereas the corresponding residues from Ubp6 are shown in parentheses. The coloring scheme for USP14 is the same as in Figure 1. Ubp6 is shown in gray. Catalytic triad residues and the oxyanion-coordinating residue are shown. Hydrogen bonds are represented by red dashed lines.

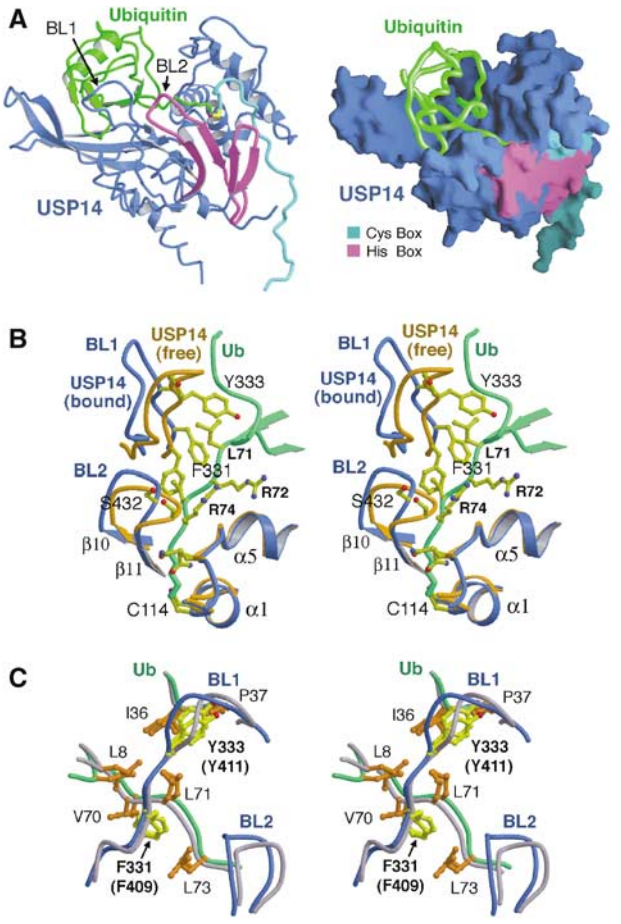

Figure 4 Structure of the USP14–Ubal complex. (**A**) Overall structure of the catalytic core domain of USP14 (91–494, blue) covalently bound to Ubal (in green). The Cys and His Boxes are colored cyan and magenta, respectively. The catalytic Cys114 is shown in a ball-and-stick representation. (**B**) A large conformational change near the active site induced by Ubal binding. The ubiquitin C-terminus-binding region of USP14 in isolation (in orange) and that in complex with Ubal (in blue) are superimposed and shown in stereo. The C-terminal tail of Ubal is shown in green. Note the conformational changes on the two surface loops, which allow the opening of the binding cleft for the C-terminus of ubiquitin. Amino acids are shown in ball-and-stick representation. (**C**) Comparison of the conformation of the blocking loops in USP14 and in HAUSP. Two conserved residues from USP14, Phe331 and Tyr333 (Phe409 and Tyr411 in HAUSP), make van der Waals interactions with residues in Ubal. The BL1/BL2 loops and Ubal in the USP14–Ubal complex are colored blue and green, respectively. The HAUSP–Ubal complex is colored gray. The side chains from USP14/HAUSP and Ubal are shown in yellow and orange, respectively.

inhibitor of most DUBs as it forms a thiohemiacetal with the catalytic cysteine, mimicking a reaction intermediate (Pickart and Rose, 1985; Hershko and Rose, 1987; Johnston *et al*, 1999). To further elucidate the catalytic mechanism of USP14, we prepared Ubal and reconstituted a covalent complex between USP14 and the inhibitor. We crystallized this binary complex and determined its structure at 3.5 Å resolution by molecular replacement (Table I). There is one USP14–Ubal complex in each asymmetric unit.

As anticipated, Ubal binds to the predicted ubiquitin-binding surface of USP14 (Figure 4A). The C-terminus of ubiquitin is covalently bonded to the deep catalytic cleft between the Palm and Thumb domains of USP14 via a

thiohemiacetal linkage between the Ubal aldehyde group and the side chain of USP14 Cys114. Binding by Ubal induces several prominent conformational changes in the catalytic domain, resulting in an RMSD of 1.3 Å for 325 aligned Cα atoms between the free and Ubal-bound USP14 structures. The recognition between USP14 and Ubal closely resembles that between HAUSP and Ubal (Hu *et al*, 2002).

Conformational changes in the active site region

Structural comparison between free USP14 and USP14 bound to Ubal revealed that the two surface loops (BL1 and BL2) that hover above the catalytic cleft of free USP14 undergo considerable conformational changes (Figure 4B). These changes significantly widen the binding groove for the C-terminus of ubiquitin. Structural overlay reveals that the aromatic side chain of Tyr333 in free USP14, which would otherwise sterically clash with Leu71 of the C-terminus of ubiquitin in the USP14–Ubal structure, undergoes a 4 Å translation and a 90° rotation upon binding to Ubal (Figure 4B). In addition, Phe331 and Ser 432 in free USP14, which would otherwise clash with Leu73 and Arg74 of ubiquitin, respectively, are translocated over a distance of 3–5 Å. These concerted changes result in the accommodation of the C-terminus of ubiquitin in the newly formed cleft between the Palm and the Thumb domains, thus allowing access of the C-terminal glycyl carbonyl of ubiquitin to the catalytic cysteine Cys114 (Figure 4B).

The conformational changes of the BL1 and BL2 loops are facilitated by interactions between conserved residues in these loops and the bound ubiquitin moiety. For example, Phe331 in USP14 makes multiple van der Waals contacts to a hydrophobic surface patch formed by Leu8, Val70, Leu71, and Leu73 of the ubiquitin moiety (Figure 4C). Tyr333 in USP14 also contacts the hydrophobic residues Ile36 and Pro37 of the ubiquitin moiety (Figure 4C). The interactions mediated by these residues, which block ubiquitin binding in the unliganded USP14, serve to stabilize ubiquitin association. Interestingly, both Phe331 and Tyr333 are conserved in HAUSP (Phe409 and Tyr411) where they make very similar interactions to stabilize substrate binding (Figure 4C) (Hu *et al*, 2002). Thus, these interactions provide a plausible explanation to the fact that portions of the BL1 sequences are conserved between USP14 and HAUSP (Figure 2). However, unlike in free USP14, the polypeptide segment corresponding to BL1 does not block the binding cleft for ubiquitin C-terminus in unliganded HAUSP (Hu *et al*, 2002). In the Ubal-bound USP14, the BL1 and BL2 loops shift to positions that are comparable to those seen in the structure of the Ubal-bound HAUSP (Hu *et al*, 2002).

Although USP14 and HAUSP share a conserved three-domain architecture, they exhibit quite distinct active site conformations and different activation mechanisms. In free HAUSP, the binding pocket for ubiquitin C-terminus is well formed; however, the catalytic triad residues are mis-aligned and undergo realignment upon binding to ubiquitin (Hu *et al*, 2002). In contrast, the catalytic triad residues are already poised for catalysis in free USP14; however, the binding groove for the C-terminus of ubiquitin is partially filled by two surface loops that undergo significant conformational changes upon binding to ubiquitin. Both mechanisms serve to activate the deubiquitinating activity and appear to ensure appropriate substrate specificity. For USP14, it is possible that association with the 26S proteasome facilitates the relief of the steric hindrance posed by the two surface loops, which in turn results in the activation of its deubiquitinating activity. To test this hypothesis, we generated 12 mutant constructs for USP14 that contained missense mutations in the BL1/BL2 region or deletion in BL1, BL2, or both. In contrast to WT USP14, none of these bacterially expressed mutant proteins was soluble (data not shown).

Disassembly of polyubiquitin chain

Most protein substrates targeted for proteasome degradation are conjugated to polyubiquitin chains (Thrower *et al*, 2000; Pickart and Cohen, 2004). USP14 is thought to play an important role in removing the ubiquitin moiety from polyubiquitinated substrates. However, the substrate specificity for USP14 remains unclear. Among the several unanswered questions, it is not known whether USP14 prefers to cleave the proximal ubiquitin from the polyubiquitin chain, or whether it instead progressively shortens polyubiquitin chains from the distal end.

To examine this aspect of substrate specificity of USP14 for polyubiquitin disassembly, we reconstituted an *in vitro* deubiquitination assay using Lys48-linked Ub_3 as a model substrate, and monitored temporal appearance of cleavage products (Figure 5A). In this triUb substrate, ubiquitin at the proximal end is fluorescently labeled by Lucifer Yellow. In the initial stage of reaction, the major deubiquitination products were found to be fluorescently labeled diubiquitin (Figure 5A) and unlabeled monoubiquitin (invisible at the 1 h time point in Figure 5A). As the reaction proceeded to completion, the fluorescently labeled diubiquitin was further reduced to monoubiquitin. Although the data shown here (Figure 5A) were obtained using the full-length USP14, similar results were obtained for the Ubl-deleted USP14 (residues 91–494, data not shown). This observation indicates that USP14 prefers to cleave ubiquitin from the distal end of a Lys48-linked polyubiquitin chain. This conclusion was also confirmed using Lys48-linked Ub_4 and Ub_5 as model substrates (data not shown). We also tested whether USP14 can cleave alternatively linked ubiquitin oligomers such as Lys63-linked diubiquitin. The cleavage was extremely slow and was almost at the detection limit (data not shown); hence, we concluded that Lys63-linked ubiquitin oligomers were unlikely to be substrates for USP14.

Association with the proteasome

USP14 was previously reported to associate with the 26S proteasome (Borodovsky *et al*, 2001), but the exact mechanism of recognition was not elucidated. To further characterize this interaction between USP14 and the proteasome, we purified fusion proteins between glutathione *S*-transferase (GST) and the full-length USP14 protein, the Ubl domain, or the catalytic domain. Then, we examined their interaction with the proteasome in a GST-mediated pull-down assay. After extensive wash, the bound proteasome was eluted using 10 mM reduced glutathione and detected by an antibody specific for the proteasomal S1 subunit. Both full-length USP14 and the Ubl domain bound efficiently to the 26S proteasome (Figure 5B). In contrast, no significant binding was detected between the catalytic domain of USP14 and the proteasome. The USP14-binding site in the proteasome was further mapped to the 19S regulatory particle (RP) of the

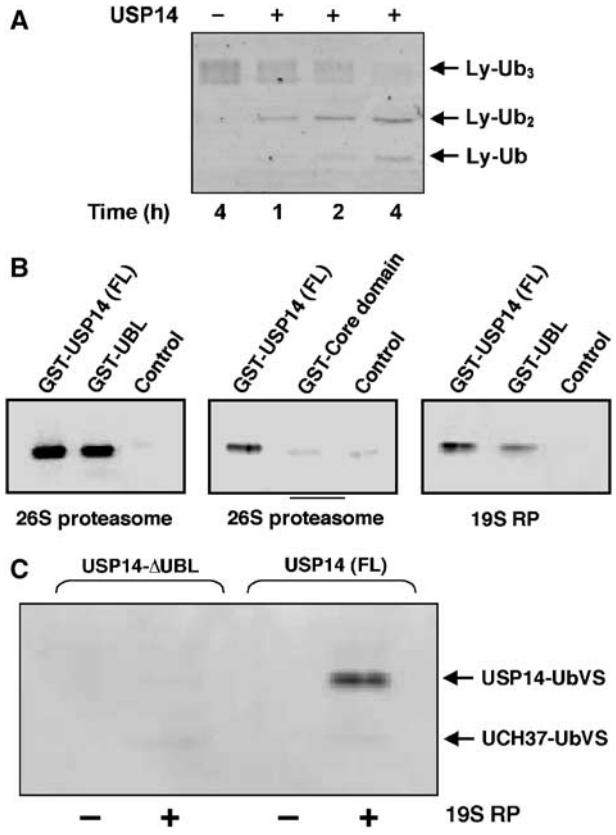

Figure 5 USP14 interacts with the 19S RP of the 26S proteasome and is activated upon binding. (**A**) Polyubiquitin chain disassembly by USP14. The proximal end ubiquitin of the triUb chain is fluorescently labeled. As indicated by the sequential appearance of fluorescent bands corresponding to labeled diUb and monoUb, USP14 preferentially cleaves ubiquitin from the distal end of the triUb chain. (**B**) The Ubl domain of USP14 is responsible for binding to the 19S RP of the 26S proteasome. An approximately equimolar amount of GST-USP14, GST-USP14 (91–494), GST-UBL, or GST (control) was used for each experiment. An equal amount of 26S proteasome or the 19S complex (PA700) was used within the same set of experiments. Only full-length (GST-USP14 (FL)) or the isolated Ubl domain (GST-UBL), but not Ubl-deleted USP14 (GST-Core domain), exhibited binding in GST pull-down assays. Anti-S1 antibody was used to detect 26S proteasome or 19S RP complexes that were bound and then eluted with glutathione (see Materials and methods). (**C**) USP14 exhibits a significant reactivity with UbVS in the presence of the 19S RP; similar results were obtained with 26S proteasomes (not shown).

proteasome, as both full-length USP14 and the Ubl domain specifically bound to the 19S RP (Figure 5B) but not the 20S proteasome catalytic core particle (not shown). The binding efficiency of full-length USP14 to the 19S RP appears to be higher than that of the Ubl domain, suggesting that additional interaction may involve the catalytic domain. These findings are consistent with the reported observations that, in yeast, the full-length Ubp6 associates with proteasomes more efficiently than the Ubl domain alone (Leggett *et al*, 2002; Chernova *et al*, 2003).

Activation of USP14 by the proteasome

UbVS is a specific covalent inhibitor of a large subset of DUBs, and thus can be used as an active site-directed probe for the detection of DUB activity (Borodovsky *et al*, 2001). In order to examine the effect of proteasome association on the activity of USP14, the purified recombinant USP14 proteins were preincubated with or without the 19S RP and then assayed for covalent modification by UbVS.

The USP14-ΔUBL protein, which lacks the ability to bind to proteasome, showed extremely low activity toward UbVS, both in the absence and presence of the 19S RP (Figure 5C, lanes 1 and 2). The full-length USP14 by itself also exhibited extremely low activity toward UbVS, as there was no detectable USP14–UbVS complex formation (Figure 5C, lane 3). However, addition of the 19S RP to the full-length USP14 sample greatly increased its activity toward UbVS, as indicated by the appearance of a strong USP14–UbVS band (Figure 5C, lane 4).

Relative to the USP14 adduct, only a trace amount of UCH37–UbVS was detected in reactions in the presence of 19S RP (Figure 5C, lanes 2 and 4). Two factors contribute to this observation. First, UCH37 appears to be intrinsically less reactive with UbVS than is the activated form of USP14; notably, this is despite the higher activity shown by UCH37 with the substrate ubiquitin-AMC (L Song and RE Cohen, unpublished observations). Second, whereas UCH37 was present in the reactions as a stoichiometric component of the 19S RP complex (Lam *et al*, 1997), USP14 was in a 22-fold molar excess. The results suggest that USP14 (and the USP14–UbVS adduct) can exchange between the populations of free and proteasome-bound enzyme.

Six ATPases are prominent among the subunits of the 19S RP (Pickart and Cohen, 2004), and therefore we tested whether USP14 activation requires ATP binding or hydrolysis. No differences in reactivity with UbVS were observed when reactions that contained 1 mM ATP were compared with those in which ATP was depleted by apyrase (data not shown). The state of the proteasome catalytic chamber may also influence USP14 activity. This possibility was suggested by the observation that treatment of cultured mammalian cells with any of several irreversible proteasome inhibitors facilitated labeling of USP14 by UbVS in cell extracts (Borodovsky *et al*, 2001). However, when we compared USP14 activation *in vitro* by 26S proteasomes preincubated with either 0 (control) or 4 μM epoxomycin, both samples showed equal reactivity with UbVS; assays with the fluorogenic peptide substrate *N*-succinyl-LLVY-7-amino-4-methylcoumarin confirmed that the proteasomes were inhibited completely by the epoxomycin (data not shown). Thus, the reported effect of proteasome inhibitors *in vivo* on USP14 activation is most likely indirect and might have been due to increased amounts of either total or proteasome-associated USP14.

The above results show that, as assessed by reaction with UbVS, USP14 activation is a consequence of binding to the 19S RP and is independent of the ATPase activities and the 20S proteolytic core of the proteasome. Thus, the simplest mechanism to explain USP14 activation is that interactions with subunit(s) in the 19S RP complex promote movement of loops BL1 and BL2 to make the active site cleft accessible to ubiquitin. This mechanism shares features with DUBs of the UCH family, which similarly have a loop that occludes the active site (Johnston *et al*, 1999; Misaghi *et al*, 2005). However, the UCHs are fundamentally different in that a single loop blocks the active site by crossing over it rather than flanking and narrowing the cleft. Moreover, the active site crossover loop residues in the UCH enzymes appear to

control activity by interfering with binding of the ubiquitin-conjugated protein or peptide rather than the ubiquitin moiety itself (Johnston *et al*, 1999; Misaghi *et al*, 2005). Whereas loop conformation may switch USP14 between ubiquitin binding and nonbinding states (active and inactive states, respectively), the active site crossover loop in UCH enzymes instead may act as a filter that can discriminate among different ubiquitin conjugates.

Discussion

It was recently reported that the Fingers domain of HAUSP resembles a zinc ribbon that has lost its zinc-binding ability (Krishna and Grishin, 2004). This class of zinc ribbon motifs has a characteristic sequence of $CX_2CX_nCX_2C$, in which the four Cys residues coordinate one zinc atom. In HAUSP, the second, third, and fourth cysteines are replaced by Val, Ala, and His, respectively, and thus zinc is not bound (Hu *et al*, 2002) (Figure 2). In USP14 and Ubp6, except for the first Cys in USP14, all other Cys positions of the motif are occupied by amino acids that cannot coordinate the zinc atom (Figure 2). Thus, although the Fingers domains in these proteins adopt a fold similar to the C_4-type zinc ribbon (Krishna and Grishin, 2004), they do not bind to zinc. Apparently, zinc binding is not generally required for deubiquitination by UBP family DUBs. Nonetheless, some UBP proteins, such as yeast Ubp8 and Doa4, contain all four Cys residues and are expected to coordinate a zinc atom.

The structures of the 45-kDa catalytic domain of USP14 in isolation and in a complex with Ubal reveal two important findings. First, USP14 indeed contains a three-domain architecture and, like the DUB HAUSP, binds to ubiquitin using the Fingers domain and the surface groove between the Palm and the Thumb. Nonetheless, it is important to note that significant local structural differences exist between HAUSP and USP14. Second, despite the conservation of this three-domain architecture, the activation mechanism for USP14 appears to be quite different from that for HAUSP. Thus, blocked active sites or mis-aligned catalytic triads seem to be a common theme for many DUBs, including not just UBPs (Hu *et al*, 2002; this study) but also UCHs (Johnston *et al*, 1999; Misaghi *et al*, 2005). It may be vital to control access to these sites in cells, as the catalytic activity of DUBs at inappropriate places or times can lead to unintended deubiquitination. It is worth noting that this conclusion is also supported by the structure of the Ubp6 catalytic core domain (www.rcsb.org, accession code 1VJV), which shows a blocked active site by two loops that are very similar to the BL1 and BL2 loops. In addition, our biochemical data show that the Ubl domain of USP14 is responsible for binding to the proteasome and that this binding is required for the activation of the deubiquitinating activity of USP14. Comparison of free and Ubal-complexed USP14 further suggests a mechanism for activation: proteasome association promotes displacement of two polypeptide loops in USP14 that otherwise block access of substrates to the active site.

How might inhibition by BL1 and BL2 be relieved by the proteasome? Although a conclusive answer remains to be experimentally investigated, we speculate that binding of the Ubl domain in USP14/Ubp6 by the proteasome brings the isopeptidase domain of USP14/Ubp6 close to specific subunit(s) of the proteasome, which promotes interactions between the BL1/BL2 loops and the proteasome subunits. These interactions in turn relieve the blockade by the BL1/BL2 loops. Alternatively, the binding of the Ubl domain in USP14/Ubp6 by the proteasome may create a novel surface that serves to interact with and change the conformation of the BL1/BL2 loops.

At present, structural information is available on only two UBP proteins (HAUSP and USP14) and their complexes with Ubal, which reveal two quite different activation mechanisms. In the case of HAUSP, the active site conformation is realigned through substrate binding; in the case of USP14, two surface loops (BL1 and BL2) are displaced to widen the binding groove for the ubiquitin C-terminus. It is entirely possible that continued biochemical and structural investigation will reveal additional novel mechanisms for the activation of the active sites in UBPs. For example, ubiquitin binding by the Fingers domain could be a regulated event, and the concave surface of the Fingers domain might be occupied by the N- or C-terminal polypeptide that extends from the isopeptidase domain of a UBP. Alternatively, these N- or C-terminal extensions could directly interact with the isopeptidase domain to deform its active site or ubiquitin-binding site. Structural investigation of the UBPs and their cognate complexes with substrate is bound to reveal additional insights into their functions and mechanisms.

Materials and methods

Protein preparation

All constructs were generated using a standard PCR-based cloning strategy. For crystallization purpose, the catalytic core domain of USP14 (91–494) was cloned into the vector pET-15b (Pharmacia), and was overexpressed in *Escherichia coli* strain BL21(DE3) as an N-terminally His_6-tagged protein. Seleno-Met-substituted USP14 (91–494) was expressed in *E. coli* B834(DE3) (Novagen) in M9 minimal medium supplemented with 50 mg l^{-1} selenomethionine. For *in vitro* deubiquitination assay using Ly-Ub_3, the full-length USP14 was cloned into pET-15b (Pharmacia), overexpressed in BL21(DE3) as an N-terminally His_6-tagged protein. For proteasome association and activation assays, the full-length USP14 and USP14 (91–494) were cloned into the vector pGEX-2T (Pharmacia), and the USP14 ubiquitin-like domain (UBL; residues 1–90) was cloned into the vector pGEX-4T-1 (Pharmacia). Protein purification followed the general procedure described (Hu *et al*, 2002).

Generation of Ubal and a USP14–Ubal complex

Ubal was prepared by carboxypeptidase Y-catalyzed exchange of 3-amino-1,2-propanediol for ubiquitin Gly76 and the subsequent oxidation of the ubiquitin-diol product with $NaIO_4$. The Ubal thus obtained was incubated in four-fold excess over USP14 (91–494) protein at pH 8 (25 mM Tris, 100 mM NaCl, 5 mM DTT), and the USP14–Ubal complex was isolated by gel filtration (Superdex 200, 10 mM Tris pH 8.0, 100 mM NaCl, 4 mM DTT).

Crystallization and data collection for free USP14

Crystals were grown by the hanging-drop method by mixing the USP14 protein (residues 91–494) ($\sim$15 mg/ml) with an equal volume of reservoir solution containing 100 mM MES pH 6.5, 200 mM $(NH_4)_2SO_4$, and 30% PEGMME 5000 (w/v). Small crystals appeared overnight and were used as seeds to generate larger crystals from Seleno-Met USP14 protein. The crystals belong to the space group P212121, with $a = 82.29$ Å, $b = 121.58$ Å, and $c = 166.85$ Å. Crystals were equilibrated in a cryoprotectant buffer containing reservoir buffer plus 20% glycerol (v/v) and were flash frozen in a cold nitrogen stream at -170°C. The native and MAD date sets were collected at NSLS beamline X-25 and CHESS F-2, respectively, and were processed using the software Denzo and Scalepack (Otwinowski and Minor, 1997).

Structure determination of free USP14

Out of the 39 selenium sites, 18 were determined using SOLVE (Terwilliger and Berendzen, 1996) and the initial experimental phases were calculated and improved by solvent flattening using DM (Collaborative Computational Project, 1994). The electron density map allowed the manual identification and docking of three copies of HAUSP catalytic domain (Hu *et al*, 2002), a homolog of USP14. After rigid-body refinement, the noncrystallographic symmetry between the three molecules allowed the identification of 30 selenium atoms from the 18 sites determined by SOLVE. The atomic model was built using O (Jones *et al*, 1991) and refined using CNS (Brunger *et al*, 1998). The heavy atom parameters were refined and new experimental phases were calculated with CNS. Three more selenium sites were determined by anomalous difference Fourier synthesis using diffraction data at the peak wavelength. After completing the heavy atom model, the new experimental phases were extensively improved by three-fold NCS averaging and extended to 3.2 Å in DM. The electron density map after DM was clear and continuous in most parts of the molecules. The final model contains three molecules in each asymmetric unit, each containing amino acids 99–216, 235–379, and 398–483. The average *B*-factor is 123.4 $Å^2$ for all atoms and the estimated coordinate error is 0.54 Å. No residue is in the disallowed region of the Ramachandran plot. There is no significant electron density for residues 94–98, 217–234, 380–397, and 484–494; these residues are likely flexible and disordered in the crystals.

Crystallization and structure determination of the USP14–Ubal complex

Crystals were grown by the hanging-drop method by mixing the complex (~10 mg/ml) with an equal volume of reservoir solution containing 100 mM Tris pH 8.0, 100 mM $CaCl_2$, and 25% PEG1000. The crystals belong to the space group P3121, with $a = b = 183.9$ Å and $c = 45.7$ Å. The native date set was collected at CHESS A-1, and processed using the software Denzo and Scalepack (Otwinowski and Minor, 1997). The structure was determined by molecular replacement using AMoRe (Navaza, 1994) and refined using CNS (Terwilliger and Berendzen, 1996). The average *B*-factor is 93.4 $Å^2$ for all atoms and the estimated coordinate error is 0.81 Å. No residue is in the disallowed region of the Ramachandran plot.

In vitro deubiquitination assays

K48-linked triubiquitin labeled with Lucifer Yellow at the proximal ubiquitin (Ly-Ub_3) was made from Ub-Ub-Ub(T66C), as described previously (Lam *et al*, 1997). To examine the substrate specificity of USP14, recombinant full-length USP14 (6 nM, or none in a control reaction) was incubated with 2 μM Ly-Ub_3 in the reaction buffer containing 50 mM HEPES pH 8.0, 50 mM NaCl, 1 mM EDTA, 5 mM DTT, and 0.1 mg/ml ovalbumin, at 37°C for the indicated time. The disassembly of fluorescent Ly-Ub_3 was visualized with a cooled CCD camera system (BioChemi System, UVP BioImaging) after separation by SDS–PAGE. Products of incubations with K63-linked polyubiquitin chains (a gift from C Pickart, Johns Hopkins University, Baltimore) were evaluated by SDS–PAGE followed by silver staining or detection after transfer to nitrocellulose with mouse monoclonal anti-ubiquitin antibody (clone P4D1; Santa Cruz).

In vitro proteasome association assay

26S proteasome purified from bovine erythrocytes was available from a previous study (Yao and Cohen, 2002). The bovine 19S complex (PA700) was a gift from G DeMartino (UT Southwestern Medical Center, Dallas). An approximately equimolar amount (0.35 nmol) of GST-USP14, GST-USP14 (91–494), GST-UBL, or GST (control) was mixed with either 2.7 pmol 26S proteasome or 1.57 pmol 19S complex (PA700) in the binding assay buffer containing 50 mM Tris pH 7.5, 1 mM ATP, 1 mM $MgCl_2$, 10 mM DTT, 0.1 mg/ml ovalbumin, and 10% glycerol. The mixture was incubated with glutathione Sepharose resin at 4°C for 1 h, followed by extensive wash using the binding assay buffer. Proteins bound to the resin were eluted with 10 mM reduced glutathione in 50 mM Tris, pH 8.0. Eluted proteins were resolved by 10% SDS–PAGE, transferred to nitrocellulose membrane, and probed with mouse monoclonal anti-S1 subunit antibody (Affiniti) as a marker for the 19S or 26S proteasome complex. Membrane blots were probed with anti-GST antibody to assure comparable loadings of resin with GST and GST fusion proteins.

Activation of USP14 by proteasome association

UbVS was prepared as described previously (Borodovsky *et al*, 2001). To test the activation of USP14 upon proteasome binding, 3.5 μM full-length USP14 or USP14-ΔUBL (91–494) was incubated with or without 157 nM bovine 19S complex (PA700) in the binding buffer containing 50 mM Tris pH 7.5, 1 mM ATP, 1 mM $MgCl_2$, 10 mM DTT, 0.1 mg/ml ovalbumin, and 10% glycerol, at 4°C for 1 h. UbVS was then added to the sample to give approximately 1:1 stoichiometry with the 19S complex. Incubation was continued for another hour and then stopped by the addition of 2 × SDS sample buffer. The reaction mixtures were resolved by 14% SDS–PAGE, transferred to nitrocellulose membrane, and the UbVS adducts were detected with mouse monoclonal anti-ubiquitin antibody (P4D1) (Santa Cruz).

Acknowledgements

We thank A Saxena at NSLS-X12C and M Becker at NSLS-X25 for help. Atomic coordinates of USP14 and the USP14–Ubal complex have been deposited with the Protein Data Bank with accession numbers 2AYN and 2AYO.

References

Amerik AY, Hochstrasser M (2004) Mechanism and function of deubiquitinating enzymes. *Biochim Biophys Acta* **1695:** 189–207

Borodovsky A, Kessler BM, Casagrande R, Overkleeft HS, Wilkinson KD, Ploegh HL (2001) A novel active site-directed probe specific for deubiquitylating enzymes reveals proteasome association of USP14. *EMBO J* **20:** 5187–5196

Brunger AT, Adams PD, Clore GM, Delano WL, Gros P, Grosse-Kunstleve RW, Jiang JS, Kuszewski J, Nilges M, Pannu NS (1998) Crystallography and NMR system: a new software suite for macromolecular structure determination. *Acta Crystallogr D* **54:** 905–921

Chernova TA, Allen KD, Wesoloski LM, Shanks JR, Chernoff YO, Wilkinson KD (2003) Pleiotropic effects of Ubp6 loss on drug sensitivities and yeast prion are due to depletion of the free ubiquitin pool. *J Biol Chem* **278:** 52102–52115

Chung KK, Dawson VL, Dawson TM (2001) The role of the ubiquitin–proteasomal pathway in Parkinson's disease and other neurodegenerative disorders. *Trends Neurosci* **24:** S7–S14

Collaborative Computational Project, N (1994) The CCP4 suite: programs for protein crystallography. *Acta Crystallogr* **D50:** 760–763

D'Andrea A, Pellman D (1998) Deubiquitinating enzymes: a new class of biological regulators. *Crit Rev Biochem Mol Biol* **33:** 337–352

Glickman MH, Ciechanover A (2002) The ubiquitin–proteasome proteolytic pathway: destruction for the sake of construction. *Physiol Rev* **82:** 373–428

Guterman A, Glickman MH (2004a) Complementary roles for Rpn11 and Ubp6 in deubiquitination and proteolysis by the proteasome. *J Biol Chem* **279:** 1729–1738

Guterman A, Glickman MH (2004b) Deubiquitinating enzymes are IN/(trinsic to proteasome function). *Curr Protein Pept Sci* **5:** 201–211

Hanna J, Leggett DS, Finley D (2003) Ubiquitin depletion as a key mediator of toxicity by translational inhibitors. *Mol Cell Biol* **23:** 9251–9261

Hershko A, Ciechanover A, Varshavsky A (2000) The ubiquitin system. *Nat Med* **6:** 1073–1081

Hershko A, Rose IA (1987) Ubiquitin-aldehyde: a general inhibitor of ubiquitin-recycling processes. *Proc Natl Acad Sci USA* **84:** 1829–1833

Hu M, Li P, Li M, Li W, Yao T, Wu JW, Gu W, Cohen RE, Shi Y (2002) Crystal structure of a UBP-family deubiquitinating enzyme in

isolation and in complex with ubiquitin aldehyde. *Cell* **111:** 1041–1054
Johnston SC, Riddle SM, Cohen RE, Hill CP (1999) Structural basis for the specificity of ubiquitin C-terminal hydrolases. *EMBO J* **18:** 3877–3887
Jones TA, Zou J-Y, Cowan SW, Kjeldgaard M (1991) Improved methods for building protein models in electron density maps and the location of errors in these models. *Acta Crystallogr* **A47:** 110–119
Kim JH, Park KC, Chung SS, Bang O, Chung CH (2003) Deubiquitinating enzymes as cellular regulators. *J Biochem (Tokyo)* **134:** 9–18
Kraulis PJ (1991) Molscript: a program to produce both detailed and schematic plots of protein structures. *J Appl Crystallogr* **24:** 946–950
Krishna SS, Grishin NV (2004) The finger domain of the human deubiquitinating enzyme HAUSP is a zinc ribbon. *Cell Cycle* **3:** 1046–1049
Lam YA, Xu W, DeMartino GN, Cohen RE (1997) Editing of ubiquitin conjugates by an isopeptidase in the 26S proteasome. *Nature* **385:** 737–740
Leggett DS, Hanna J, Borodovsky A, Crosas B, Schmidt M, Baker RT, Walz T, Ploegh H, Finley D (2002) Multiple associated proteins regulate proteasome structure and function. *Mol Cell* **10:** 495–507
Misaghi S, Galardy PJ, Meester WJ, Ovaa H, Ploegh HL, Gaudet R (2005) Structure of the ubiquitin hydrolase UCH-L3 complexed with a suicide substrate. *J Biol Chem* **280:** 1512–1520
Navaza J (1994) AMoRe and automated package for molecular replacement. *Acta Crystallogr* **A50:** 157–163
Nicholls A, Sharp KA, Honig B (1991) Protein folding and association: insights from the interfacial and thermodynamic properties of hydrocarbons. *Proteins Struct Funct Genet* **11:** 281–296
Otwinowski Z, Minor W (1997) Processing of X-ray diffraction data collected in oscillation mode. *Methods Enzymol* **276:** 307–326
Papa FR, Amerik AY, Hochstrasser M (1999) Interaction of the Doa4 deubiquitinating enzyme with the yeast 26S proteasome. *Mol Biol Cell* **10:** 741–756
Papa FR, Hochstrasser M (1993) The yeast DOA4 gene encodes a deubiquitinating enzyme related to a product of the human tre-2 oncogene. *Nature* **366:** 313–319
Pickart CM (2004) Back to the future with ubiquitin. *Cell* **116:** 181–190
Pickart CM, Cohen RE (2004) Proteasomes and their kin: proteases in the machine age. *Nat Rev Mol Cell Biol* **5:** 177–187
Pickart CM, Rose IA (1985) Ubiquitin carboxyl-terminal hydrolase acts on ubiquitin carboxyl-terminal amides. *J Biol Chem* **260:** 7903–7910
Schwartz AL, Ciechanover A (1999) The ubiquitin–proteasome pathway and pathogenesis of human diseases. *Annu Rev Med* **50:** 57–74
Terwilliger TC, Berendzen J (1996) Correlated phasing of multiple isomorphous replacement data. *Acta Crystallogr D* **52:** 749–757
Thrower JS, Hoffman L, Rechsteiner M, Pickart CM (2000) Recognition of the polyubiquitin proteolytic signal. *EMBO J* **19:** 94–102
Verma R, Aravind L, Oania R, McDonald WH, Yates III JR, Koonin EV, Deshaies RJ (2002) Role of Rpn11 metalloprotease in deubiquitination and degradation by the 26S proteasome. *Science* **298:** 611–615
Verma R, Chen S, Feldman R, Schieltz D, Yates J, Dohmen J, Deshaies RJ (2000) Proteasomal proteomics: identification of nucleotide-sensitive proteasome-interacting proteins by mass spectrometric analysis of affinity-purified proteasomes. *Mol Biol Cell* **11:** 3425–3439
Wilkinson CR, Ferrell K, Penney M, Wallace M, Dubiel W, Gordon C (2000) Analysis of a gene encoding Rpn10 of the fission yeast proteasome reveals that the polyubiquitin-binding site of this subunit is essential when Rpn12/Mts3 activity is compromised. *J Biol Chem* **275:** 15182–15192
Wilson SM, Bhattacharyya B, Rachel RA, Coppola V, Tessarollo L, Householder DB, Fletcher CF, Miller RJ, Copeland NG, Jenkins NA (2002) Synaptic defects in ataxia mice result from a mutation in Usp14, encoding a ubiquitin-specific protease. *Nat Genet* **32:** 420–425
Wing SS (2003) Deubiquitinating enzymes—the importance of driving in reverse along the ubiquitin–proteasome pathway. *Int J Biochem Cell Biol* **35:** 590–605
Wyndham AM, Baker RT, Chelvanayagam G (1999) The Ubp6 family of deubiquitinating enzymes contains a ubiquitin-like domain: SUb. *Protein Sci* **8:** 1268–1275
Xie Y, Varshavsky A (2000) Physical association of ubiquitin ligases and the 26S proteasome. *Proc Natl Acad Sci USA* **97:** 2497–2502
Yao T, Cohen RE (2002) A cryptic protease couples deubiquitination and degradation by the proteasome. *Nature* **419:** 403–407
Zwickl P, Voges D, Baumeister W (1999) The proteasome: a macromolecular assembly designed for controlled proteolysis. *Philos Trans R Soc London B* **354:** 1501–1511